# The posttranslational modification of tubulin undergoes a switch from detyrosination to acetylation as epithelial cells become polarized

Geraldine B. Quinones[a], Barbara A. Danowski[b], Anjan Devaraj[a], Vimla Singh[a], and Lee A. Ligon[a]
[a]Department of Biology and Center for Biotechnology and Interdisciplinary Studies, Rensselaer Polytechnic Institute, Troy, NY 12180; [b]Union College, Schenectady, NY 12308

**ABSTRACT** **Tubulin posttranslational modifications (PTMs) have been suggested to provide navigational cues for molecular motors to deliver cargo to spatially segregated subcellular domains, but the molecular details of this process remain unclear. Here we show that in Madin-Darby Canine Kidney (MDCK) epithelial cells, microtubules express several tubulin PTMs. These modifications, however, are not coordinated, and cells have multiple subpopulations of microtubules that are marked by different combinations of PTMs. Furthermore these subpopulations show differential sensitivity to both drug- and cold-induced depolymerization, suggesting that they are functionally different as well. The composition and distribution of modified microtubules change as cells undergo the morphogenesis associated with polarization. Two-dimensionally polarized spreading cells have more detyrosinated microtubules that are oriented toward the leading edge, but three-dimensionally polarized cells have more acetylated microtubules that are oriented toward the apical domain. These data suggest that the transition from 2D polarity to 3D polarity involves both a reorganization of the microtubule cytoskeleton and a change in tubulin PTMs. However, in both 2D polarized and 3D polarized cells, the modified microtubules are oriented to support vectorial cargo transport to areas of high need.**

**Monitoring Editor**
Erika L. F. Holzbaur
University of Pennsylvania

Received: Jun 18, 2010
Revised: Jan 21, 2011
Accepted: Jan 28, 2011

## INTRODUCTION

As epithelial cells undergo the cellular morphogenesis associated with the development of apical–basal polarity, the microtubule cytoskeleton undergoes a dramatic rearrangement. In unpolarized epithelial cells, the microtubule cytoskeleton is typically arranged in an astral array with the minus ends anchored at the centrosome and the plus ends extending out toward the periphery. As cells become polarized, however, the microtubule network is rearranged into several spatially localized arrays of noncentrosomal microtubules which include an apical mesh, a basal mesh, and longitudinal bundles that run parallel to the long axis of the cell (Bacallao *et al.*, 1989; Müsch, 2004; Bartolini and Gundersen, 2006). It is thought that these noncentrosomal microtubules in polarized cells are more stable than the centrosomal microtubules in unpolarized cells (Bré *et al.*, 1990; Bartolini and Gundersen, 2006), but the mechanisms underlying both the network reorganization and increased microtubule stabilization remain unclear.

Tubulin subunits in stable microtubules are often modified posttranslationally, although these modifications are not thought to cause microtubule stability. These modifications include acetylation of α-tubulin on lysine-40 (L'Hernault and Rosenbaum, 1985; Piperno and Fuller, 1985), the removal of the terminal tyrosine from α-tubulin (detyrosination) (Thompson, 1977; Gundersen *et al.*, 1984), and addition of variable length chains of glutamate or glycine residues to glutamate residues near the C termini of both α- and β-tubulin (Eddé *et al.*, 1990; Redeker *et al.*, 1994) (reviewed in Hammond *et al.*, 2008). Recent data have suggested that some molecular motors can read the "code" of tubulin posttranslational modifications (PTMs) and use them like road signs to navigate the microtubule highways of the cell (Reed *et al.*, 2006; Cai *et al.*, 2009) (reviewed in Verhey and Hammond, 2009). These road signs may be particularly

This article was published online ahead of print in MBoC in Press (http://www.molbiolcell.org/cgi/doi/10.1091/mbc.E10-06-0519) on February 9, 2011.

Address correspondence to: Lee A. Ligon (ligonl@rpi.edu).

Abbreviations used: DMSO, dimethyl sulfoxide; FT, flow-through; IP, immunoprecipitate; MDCK, Madin-Darby Canine Kidney; PBS, phosphate-buffered saline; PTMs, posttranslational modifications; TSA, trichostatin A.

important in spatially complex cells like neurons where cargo must be delivered to and from distinct subcellular domains that are often separated by significant distance. For example, motors of the kinesin-1 family appear to be able to use tubulin PTMs to navigate specifically to the axonal domain, and this is thought to be a key factor in the establishment and maintenance of neuronal polarity (Jacobson *et al.*, 2006; Konishi and Setou, 2009; Hammond *et al.*, 2010).

Like neurons, mature epithelial cells are spatially complex with distinct subcellular domains. As in neurons, the maintenance of polarity is crucial for cellular function, and the high-fidelity trafficking of cargo to the appropriate domain is a key feature in both the establishment and maintenance of polarity. Both the major minus end–directed microtubule motor, cytoplasmic dynein, as well as a minus end–directed kinesin (kif3c—a member of the kinesin-2 family), have been shown to play a role in the delivery of apical cargoes in polarized epithelial cells (Noda *et al.*, 2001; Wang *et al.*, 2003). Most of the microtubules in these cells are arranged into longitudinal bundles with their minus ends near the apical membrane and their plus ends near the basal membrane. A minus end–directed motor, therefore, would not need specific directional cues to navigate to the apical domain. Plus end–directed motors, however, have also been suggested to transport cargoes to the apical domain. These motors include members of the kinesin-1 family, such as kif5b and kif5c (Jaulin *et al.*, 2007; Astanina and Jacob, 2010), and kif3b, a member of the kinesin-2 family (Reed *et al.*, 2010). Although there are microtubules with their plus ends oriented toward the apical domain (Jaulin *et al.*, 2007), these motors must be able to selectively target this subpopulation of microtubules. Tubulin PTMs are potential mechanisms for this targeting, but it is not clear if the expression and distribution of PTMs in these cells would support this mechanism.

To determine whether there are subpopulations of microtubules marked by tubulin PTMs in polarized epithelial cells, we have used immunoblotting and immunocytochemistry in Madin-Darby Canine Kidney (MDCK) cells at different stages of polarity. Surprisingly, we found that not only is there a subpopulation of microtubules marked by tubulin PTMs, but there are several subpopulations marked by different combinations of PTMs. It has been hypothesized that stable microtubules are good substrates for modification; therefore a stable microtubule would tend to be modified by all the modifications present in the cell. Although this may be the case in neurons (Banerjee, 2002), here we used immunoprecipitation and immunocytochemistry to show that tubulin PTMs do not completely overlap on the same microtubules in epithelial cells, providing additional evidence to suggest that these are distinct subpopulations. Furthermore we looked at the ability of these microtubule subpopulations to resist drug- and cold-induced depolymerization and showed that they differ functionally as well. Finally, these subpopulations change in composition as cells undergo polarization. In two-dimensionally polarized cells, detyrosinated microtubules that point to the leading edge of spreading cells predominate, but when cells are three-dimensionally polarized, acetylated microtubules oriented toward the apical domain predominate.

## RESULTS

### PTMs demarcate distinct subpopulations of microtubules in epithelial cells that change as cells become polarized

To determine whether the PTM of tubulin changes as epithelial cells become polarized, we grew MDCK epithelial cells to three stages in the transition to apical–basal polarity: subconfluent, confluent, and polarized. MDCK cells tend to grow as expanding islands, and, at the subconfluent stage, cells have a degree of two-dimensional polarity. Cells at the periphery of islands are in contact with neighboring cells on one side, but not the other. Furthermore the uncontacted edge has similarities to the leading edge of a migrating cell (Waterman-Storer and Salmon, 1997). When cells become confluent, they lose this two-dimensional polarity. As cells continue to divide and the packing density increases, however, they undergo a morphogenesis involving lateral compression and vertical extension that results in an epithelial sheet with three-dimensional apical–basal polarity. We prepared lysates from cells grown to each of these stages, and performed SDS–PAGE followed by immunoblotting with antibodies to α-tubulin and several PTMs of tubulin. We also prepared lysates from cells grown on permeable membrane inserts, as they have previously been shown to be an excellent model of epithelial polarity (Cereijido *et al.*, 1978).

The total amount of tubulin did not change significantly as cells became polarized, but the relative amount of modified tubulins did change, and, surprisingly, these changes were not coordinated among modifications. The proportion of tubulin that was acetylated remained relatively constant as cells underwent morphogenesis, although there was a slight decrease in the number of polarized cells. The proportion of tubulin that was detyrosinated, in contrast, was highest in subconfluent cells but dropped significantly as cells became confluent and polarized cells expressed little detyrosinated tubulin. Polyglutamylated tubulin also showed the highest level of expression in subconfluent cells, and gradually decreased as cells became more polarized, although the decrease was not significant (Figure 1, A and B). These data suggest that the relative amount of modified tubulin changes as epithelial cells become polarized and further that each individual modification changes independently of the others.

To characterize the distribution of modified microtubules in cells at different stages of polarization, we grew cells to the stages described earlier in the text and fixed and prepared them for immunocytochemistry. In subconfluent cells, labeling with an antibody to α-tubulin shows that the microtubule network is largely centrosomally organized in both cells at the edge of islands and those in the interior of islands (Figure 2A). A subpopulation of microtubules was labeled with an acetylated tubulin antibody in both edge cells and interior cells. Although there was some cell-to-cell variability in the relative amount of acetylated tubulin per cell (as determined by the ratio of acetylated tubulin labeling to α-tubulin labeling), there was no significant difference in the acetylated tubulin-to-α-tubulin ratio between edge cells and interior cells. Labeling with an antibody to detyrosinated tubulin showed that there was also a subpopulation of detyrosinated microtubules in subconfluent cells and that cells at the edge of the islands had on average 15% more detyrosinated tubulin labeling than did those in the interior of islands ($p < 0.05$). Finally, a subpopulation of microtubules was also labeled with a polyglutamylated tubulin antibody, but there was no difference in the relative amount between edge cells and interior cells.

The microtubules labeled by these three tubulin PTM antibodies also showed different distributions and morphological characteristics. Acetylated microtubules were isotropically distributed throughout most edge and interior cells, and, as has previously been described, they were more curved than were nonacetylated microtubules in the same cell (Figure 2A) (Piperno *et al.*, 1987; Friedman *et al.*, 2010). In addition, the acetylated tubulin labeling appeared to consist of short microtubule segments, but, because of the density of the microtubule network, it was not clear whether these segments were part of longer microtubules or whether they represented short microtubules. To answer this question, we treated cells with 10 μM nocodazole for 10 min (Figure 2C). This short drug treatment depolymerized many of the microtubules, but left some, including many

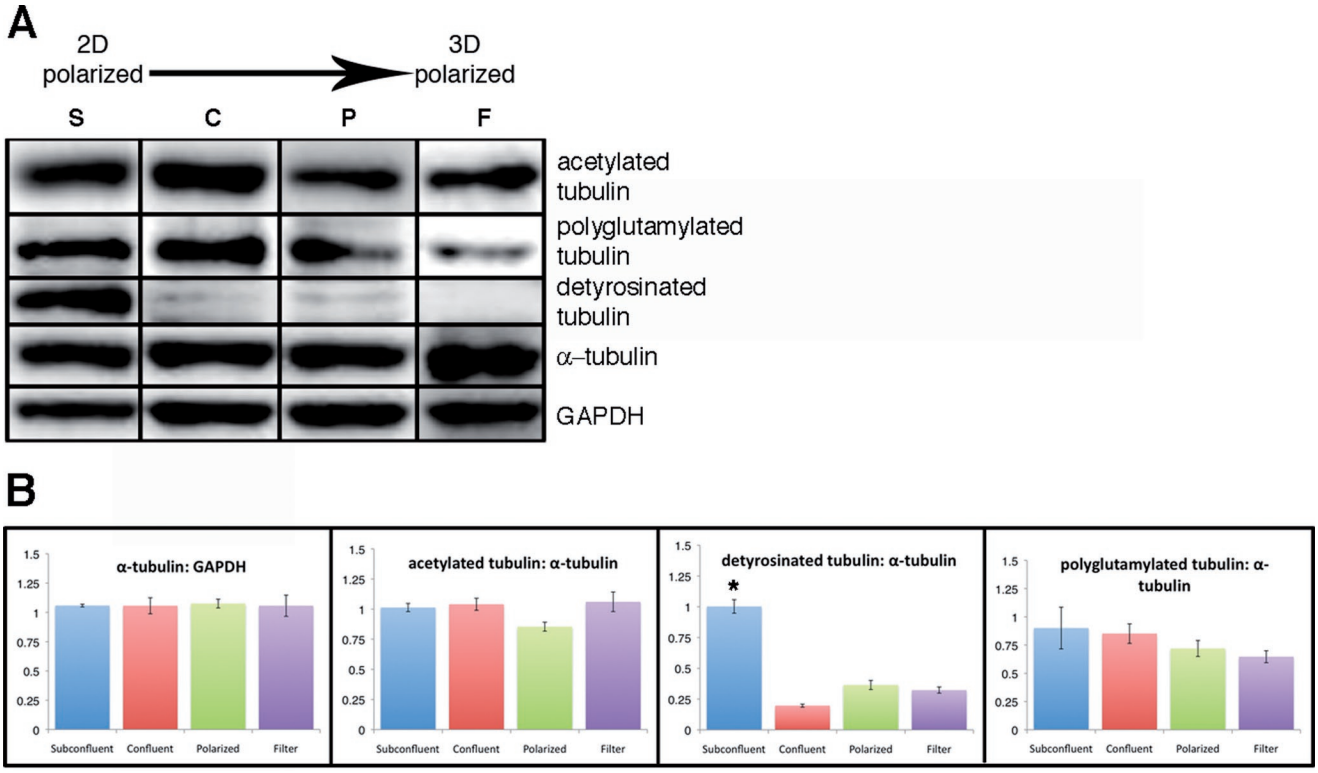


FIGURE 1: PTMs of tubulin in epithelial cells at different stages of polarity. (A) Immunoblot of lysates from MDCK cells grown to subconfluent (S), confluent (C), or polarized (P) stage or from cells grown to polarized stage on filters (F), labeled with antibodies to α-tubulin, tubulin PTMs, and GAPDH as a loading control. (B) Normalized expression levels of α-tubulin and tubulin PTMs in epithelial cells at different stages of polarization. Shown are means ± SEM (n = 3 independent lysates/stage). Pairwise student's *t* tests show that the level of detyrosinated tubulin in subconfluent cells is significantly higher than in confluent, polarized, or filter-grown cells.

with PTMs, intact. The acetylated microtubules that persisted after drug treatment had organization and distribution similar to those in control cells (Figure 2, A and C). Linescans along microtubules revealed segments of bright acetylated tubulin labeling interspersed with segments of little acetylated tubulin labeling, whereas the α-tubulin labeling was more consistent along the length of the same microtubule (Figure 2C). These data suggest that microtubules are not necessarily acetylated along their entire length, but rather the modification may be applied to short segments of microtubules, which may account for the characteristic appearance of acetylated microtubules.

Detyrosinated microtubules, in contrast, have a different appearance. In cells in the interior of islands, long microtubules were labeled, many of which appeared to wrap around the circumference of the cell. In cells on the edge of islands, the detyrosinated microtubules were prominent and tended to be long and straight and point toward the spreading edge (Figure 2A). This finding is similar to those showing that detyrosinated microtubules point toward the leading edge of migrating fibroblasts (Gundersen and Bulinski, 1988; Nagasaki *et al*., 1992). Linescans along microtubules in cells incubated briefly in nocodazole showed consistent levels of labeling along the length of the filament by both α-tubulin and detyrosinated tubulin antibodies (Figure 2C). These data suggest that, unlike acetylation, detyrosination is applied to tubulin in long stretches of microtubules.

Labeling with a polyglutamylated tubulin antibody revealed a third pattern of tubulin modification. Many of the microtubules in both edge and interior cells showed discontinuous labeling along the length of the microtubules. Linescans along microtubules in cells incubated briefly in nocodazole showed bright puncta of labeling along the length of the filament in contrast to more consistent α-tubulin labeling (Figure 2C). These data suggest that polyglutamylation may occur stochastically on tubulin in most microtubules in these cells.

The microtubule network in confluent cells was similar in overall appearance to that seen in subconfluent cells, although there were more microtubules that did not appear to originate at the centrosome (Figure 2B). The amount and distribution of acetylated microtubules in confluent cells was also similar to that seen in subconfluent cells (Figure 2B). There was less detyrosinated tubulin and polyglutamylated tubulin in confluent cells, but the general pattern of labeling was similar to that seen in subconfluent cells (Figure 2B).

The organization of the microtubule network in polarized cells, however, is significantly different from that seen in unpolarized cells (Müsch, 2004; Bartolini and Gundersen, 2006). Most of the microtubules are no longer anchored at the centrosome and are arranged into an apical mesh (see apical section, Figure 3, A–C), basal mesh (see basal section, Figure 3, A–C), and longitudinal bundles that traverse the long axis of the cell from the apical domain to the basal domain (seen in cross-section in middle section, Figure 3, A–C). In addition, a primary cilium extends from the apical domain of each cell. Detyrosinated tubulin was seen only in the primary cilia, and polyglutamylated tubulin was enriched in the primary cilia but showed a diffuse labeling throughout the cell (Figure 3, B and C). Acetylated tubulin, in contrast, was enriched in the primary cilia, the apical microtubule mesh, and the longitudinal bundles (arrows, Figure 3A). Together these data suggest that, in both unpolarized

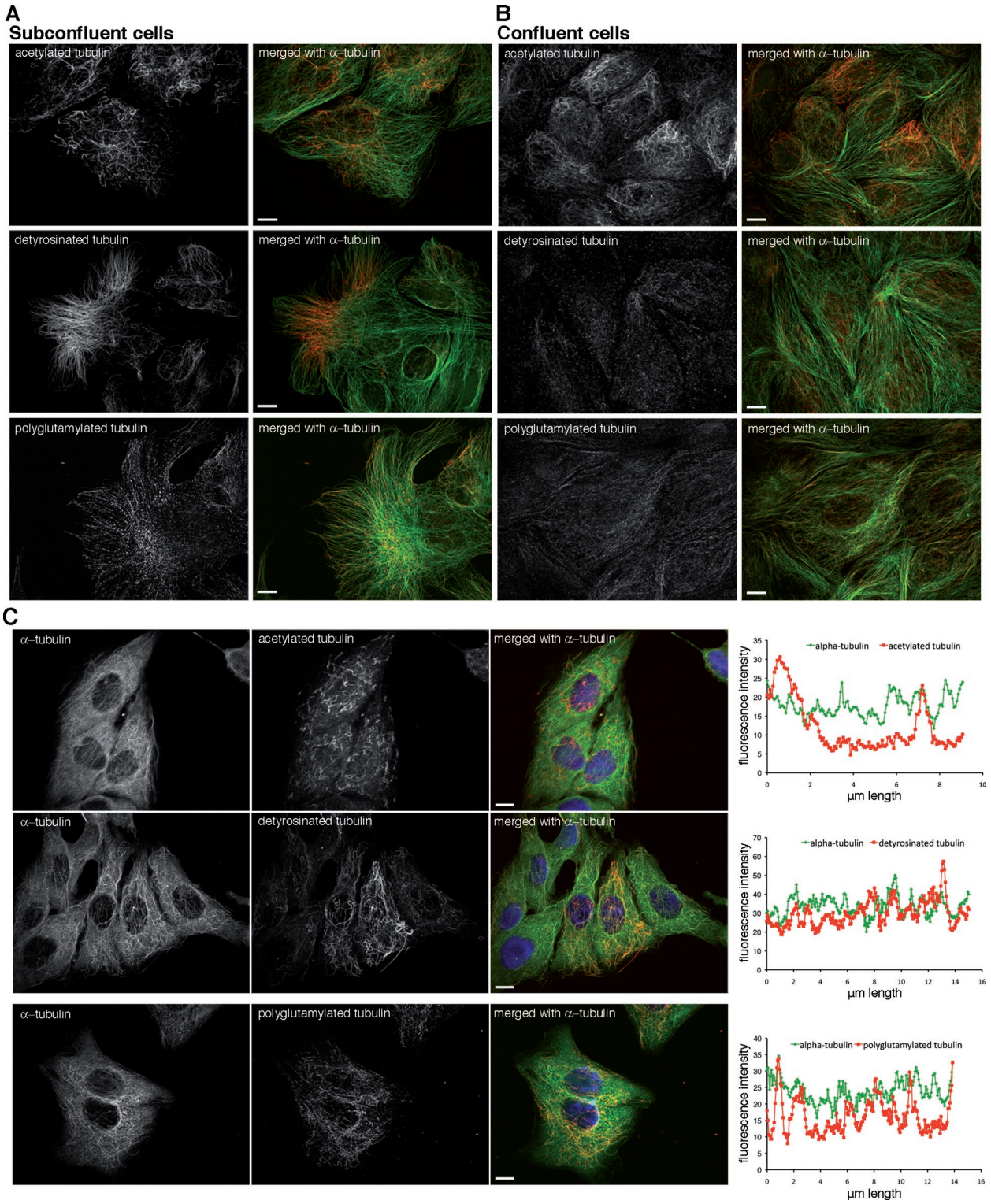


FIGURE 2: The distribution of posttranslationally modified tubulin in unpolarized epithelial cells. (A) Immunocytochemistry on subconfluent MDCK cells with antibodies to acetylated tubulin (top row), detyrosinated tubulin (middle row), or polyglutamylated tubulin (bottom row) in combination with an antibody to α-tubulin. (B) Immunocytochemistry on confluent MDCK cells with antibodies to acetylated tubulin (top row), detyrosinated tubulin (middle row), or polyglutamylated tubulin (bottom row) in combination with an antibody to α-tubulin. (C) Subconfluent cells were treated with 10 μM nocodazole for 10 min before fixation and labeling with antibodies as described earlier. Lines were traced along individual microtubules, and the fluorescence intensity profile along the line was plotted for each label. Scale = 9 μm.

and polarized epithelial cells, there are subpopulations of microtubules that are modified by acetylation, detyrosination, and polyglutamylation of tubulin subunits. The relative amount of each of these modifications, however, is different at different stages of polarity, and the microtubules marked by each of the modifications have different distributions and morphologies, suggesting that

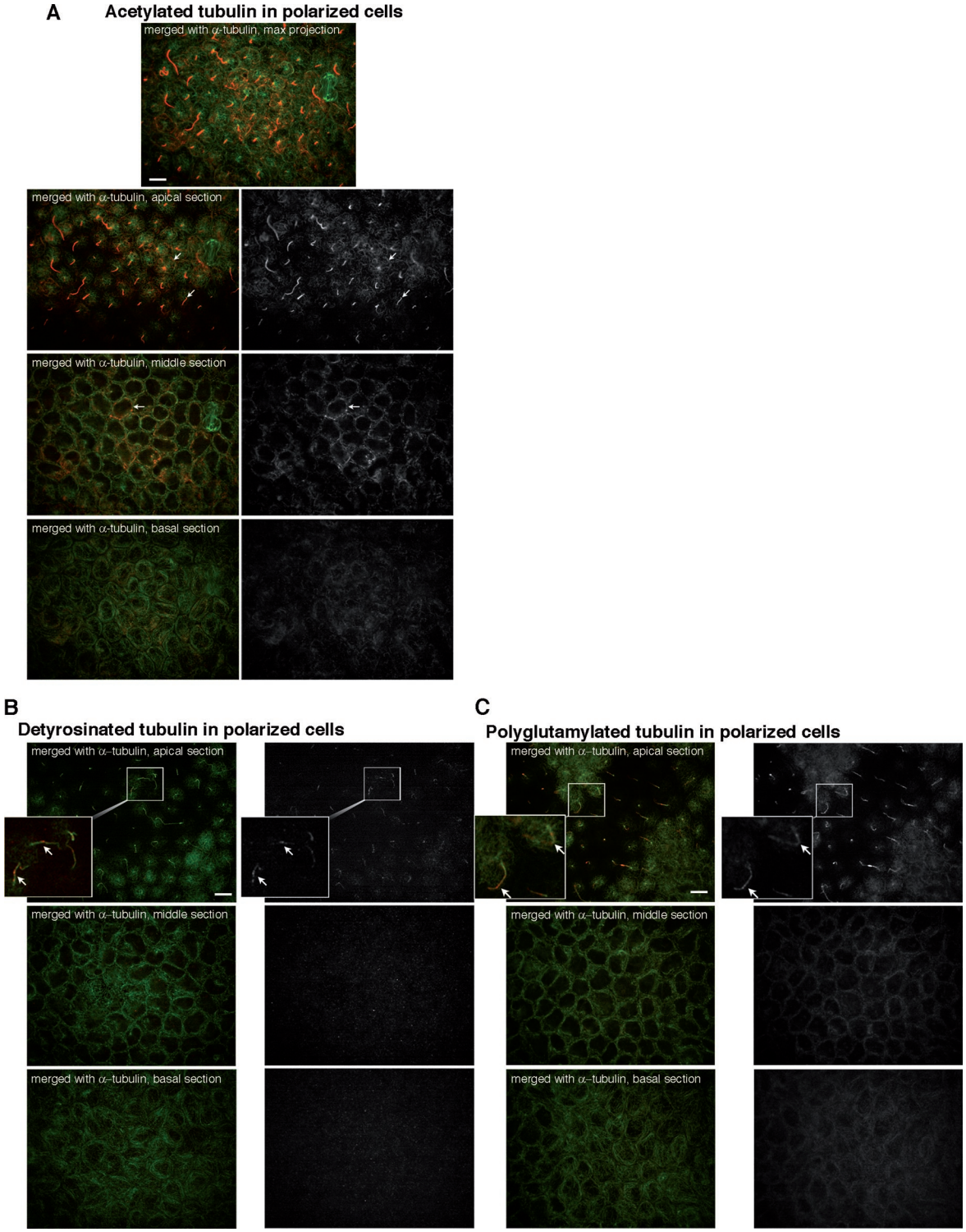


FIGURE 3: The distribution of posttranslationally modified tubulin in polarized epithelial cells. (A) Immunocytochemistry on polarized MDCK cells with antibodies to acetylated tubulin and α-tubulin. Top panel is a maximum projection image, and below are single optical sections from the apical domain, middle domain, and basal domain. Black and white panels are acetylated tubulin, and color panels are acetylated tubulin (red) merged with α-tubulin (green). Arrows show enrichment of acetylated tubulin in primary cilia, apical mesh microtubules, and lateral microtubule bundles. (B) Immunocytochemistry on polarized cells with antibodies to detyrosinated tubulin and α-tubulin showing single optical sections from the apical domain, middle domain, and basal domain. Black and white panels are detyrosinated tubulin, and color panels are detyrosinated tubulin (red) merged with α-tubulin (green). Inset shows enrichment of detyrosinated tubulin in primary cilia (arrows). (C) Immunocytochemistry on polarized cells with antibodies to polyglutamylated tubulin and α-tubulin showing single optical sections from the apical domain, middle domain, and basal domain. Black and white panels are polyglutamylated tubulin, and color panels are polyglutamylated tubulin (red) merged with α-tubulin (green). Inset shows enrichment of polyglutamylated tubulin in primary cilia (arrows). Scale = 9 μm.

these modifications may demarcate distinct subpopulations of microtubules. Furthermore these data suggest that, as epithelial cells transition from two-dimensional polarity (subconfluent) to three-dimensional polarity (polarized), the predominant tubulin modification changes from detyrosination to acetylation.

### PTMs of tubulin are not coordinated

We next asked whether the tubulin modifications were found on the same populations of microtubules. We grew cells to either the subconfluent or confluent stage and fixed and labeled them with antibodies to either acetylated tubulin and detyrosinated tubulin or polyglutamylated tubulin and detyrosinated tubulin. In both subconfluent and confluent cells, microtubules could be found that were both acetylated and detyrosinated (double arrow, Figure 4, A and B), but there were also microtubules that were only acetylated (arrowhead, Figure 4, A and B) or only detyrosinated (single arrow, Figure 4, A and B). Similarly, detyrosinated and polyglutamylated tubulin only partially overlapped as well (Figure 4, C and D). Although these observations are qualitative, they suggest that there are multiple subpopulations of microtubules, some with single PTMs and some with combinations of PTMs.

To further analyze the coordination of tubulin modifications, we immunoprecipitated acetylated tubulin and probed with antibodies to detyrosinated tubulin and polyglutamylated tubulin. At all three cell stages, all the acetylated tubulin label was in the immunoprecipitate (IP) fraction, and none remained in the flow-through (FT). In subconfluent cells, the detyrosinated tubulin partitioned approximately equally between the acetylated (IP) fraction and the nonacetylated fraction, but all the polyglutamylated tubulin coprecipitated with the acetylated tubulin (Figure 4E). In confluent and polarized cells, there appeared to be even less coordination between modified tubulins as both detyrosinated and polyglutamylated tubulin was distributed in both the acetylated and nonacetylated fractions (Figure 4E). It is not clear if the fraction in which the PTMs are coordinated represents multiple PTMs on single tubulin dimers or if it represents small aggregates of tubulin dimers each of which has different modifications; further experiments will need to be performed to assess this.

We then artificially increased the acetylation of microtubules by inhibiting one of the known tubulin deacetylases (HDAC6) with the inhibitor trichostatin A (TSA). Cells treated with TSA had more acetylated microtubules, but this did not lead to an increase in either polyglutamylated tubulin or detyrosinated tubulin (Figure 5, A and B), further indicating that these PTMs are not coupled. Together these data indicate that there is little coordination between tubulin PTMs in either unpolarized or polarized epithelial cells, suggesting that each modification is independently regulated and may serve different functions within the cell.

### Microtubules with different tubulin PTMs have different stability

To determine whether PTMs mark microtubules with different characteristics, we examined the resistance to depolymerization by either nocodazole or cold treatment. Cells were treated with 33 μM nocodazole for 1 or 2 h and then lysed and prepared for immunoblotting or fixed and prepared for immunocytochemistry with antibodies to α-tubulin and PTMs. Immunoblots show that the total amount of α-tubulin did not change after incubation in nocodazole for 1 h (lysates retain both polymerized and unpolymerized tubulin). Detyrosinated tubulin and polyglutamylated tubulin were also unchanged, but acetylated tubulin was significantly decreased after drug treatment (Figure 6, A and B). Immunocytochemistry experiments confirm that, in subconfluent cells, detyrosinated microtubules initially appeared more stable to drug-induced depolymerization than did acetylated microtubules. After 1 h of nocodazole treatment, few acetylated microtubules remained, but many cells had detyrosinated microtubules (Figure 6C). After longer drug treatment, most of the detyrosinated microtubules were depolymerized as well. Interestingly, approximately the same number of acetylated microtubules remained after 2 h of drug treatment as remained after 1 h (Figure 6C), suggesting that there may be different classes of stable microtubules in these cells—a small number of hyperstable acetylated microtubules and a somewhat larger number of detyrosinated microtubules that are initially stable but depolymerize after longer drug exposure. Whereas the immunoblots suggested that polyglutamylation was not affected by drug treatment, the immunocytochemistry experiments do not reveal any drug-resistant polyglutamylated microtubules. Bright punctate labeling with the polyglutamylated tubulin antibody, however, remained after the drug treatment, distributed throughout the cell. The largest of these puncta may be the centrosomes, but the smaller ones may be aggregates of polyglutamylated tubulin, suggesting that tubulin deglutamylation does not occur rapidly upon microtubule depolymerization, unlike tubulin deacetylation and retyrosination (Figure 6, A–C).

Resistance to nocodazole was similar in confluent cells. A small number of acetylated microtubules persisted after 1 or 2 h of drug treatment, and no polyglutamylated microtubules resisted drug treatment (Figure 6D). There are few detyrosinated microtubules in confluent cells; therefore it was impossible to assess the effect of the drug treatment on them. The microtubules in polarized cells were particularly resistant to nocodazole-induced depolymerization, and drug-resistant microtubules were seen in all regions of the cell, even after a 2-h drug incubation (Figure 6E). Most of these drug-resistant microtubules contained acetylated tubulin (Figure 6E), but detyrosinated tubulin and polyglutamylated tubulin were primarily concentrated in the microtubules of the primary cilia (unpublished data).

Although acetylated microtubules were depolymerized by nocodazole treatment, they were initially somewhat more resistant to cold-induced depolymerization than were detyrosinated microtubules. Cells were incubated at 4°C for 15, 30, or 60 min and then fixed and processed for immunocytochemistry with antibodies to α-tubulin in combination with acetylated tubulin, detyrosinated ulin, or polyglutamylated tubulin. After 15 min at 4°C, most cells in subconfluent cultures still had several microtubules containing detyrosinated tubulin, but significantly more with acetylated tubulin. After 30 min, however, most of the acetylated microtubules were depolymerized, although a few detyrosinated microtubules remained. All microtubules were depolymerized after 60 min at 4°C (Figure 7, A and B). Surprisingly, many of the microtubules initially resistant to cold-induced depolymerization also contained polyglutamylated tubulin (Figure 7C). Resistance to cold-induced depolymerization was similar in confluent cells. Initially some microtubules containing acetylated and polyglutamylated tubulin were resistant to cold, but with longer exposure depolymerized (Figure 8A).

The microtubules in polarized cells were resistant to cold-induced depolymerization as well as drug-induced depolymerization (Figure 8B). Most of the cold-resistant microtubules contained acetylated tubulin (Figure 8B), whereas detyrosinated tubulin was primarily concentrated in the microtubules of the primary cilia. Polyglutamylated tubulin was seen in the cold-resistant microtubules of the primary cilia but also was diffusely distributed throughout the cell. Together these data suggest that not only do PTMs demarcate

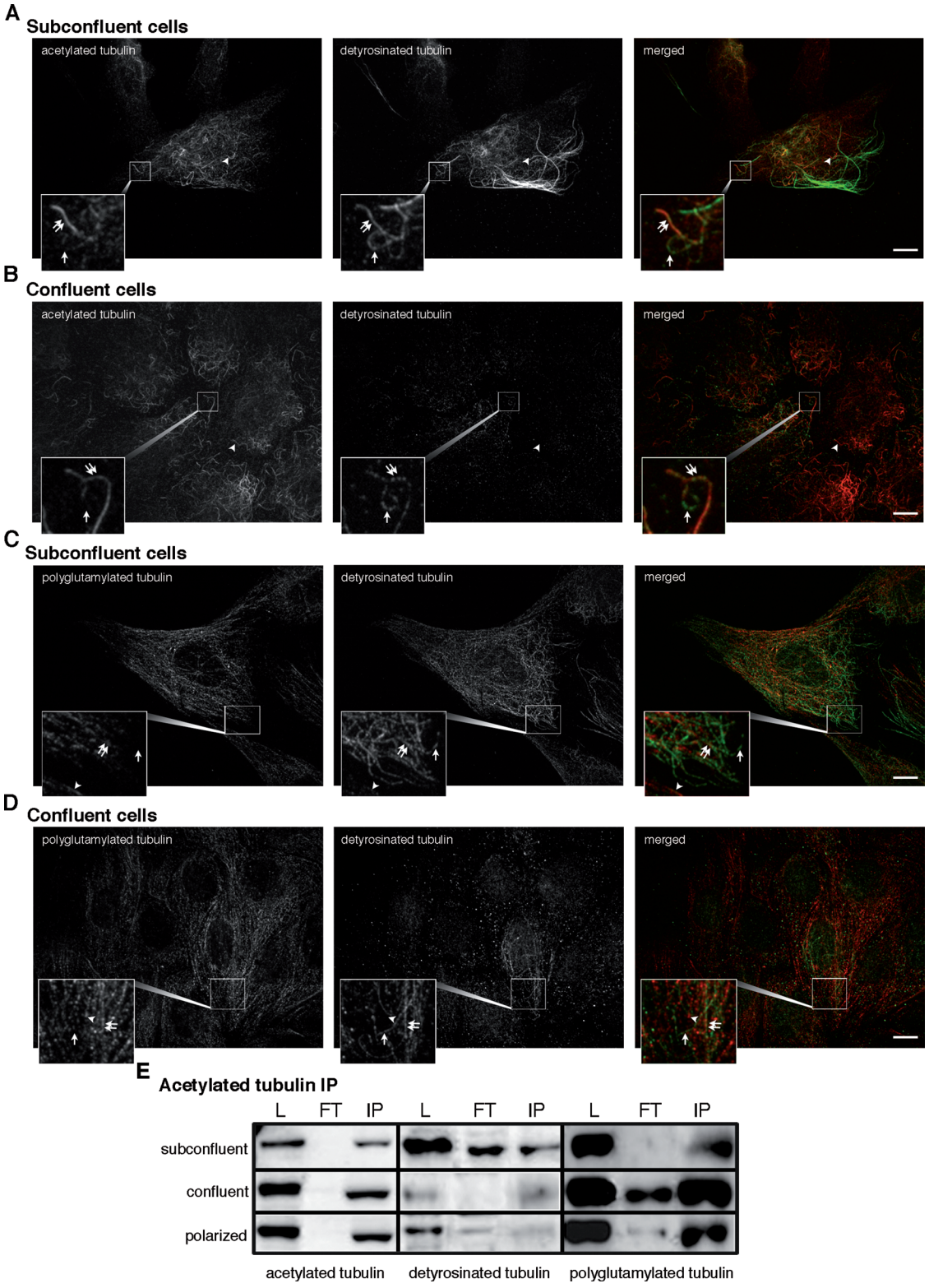


FIGURE 4: Microtubules marked by different tubulin PTMs only partially overlap in MDCK epithelial cells. Subconfluent (A and C) or confluent (B and D) cells were labeled with acetylated (red) and detyrosinated (green) tubulin antibodies (A and B) or polyglutamylated (red) and detyrosinated (green) tubulin antibodies (C and D). In all cases, representative microtubules labeled by two modifications are indicated in insets by double arrows, and representative microtubules only marked by detyrosination are indicated with arrows. Those marked by only acetylation are indicated by arrowheads in panels A and B, and those marked by only polyglutamylation are indicated by arrowheads in C and D. (E) Acetylated tubulin was immunoprecipitated from lysates from subconfluent, confluent, or polarized MDCK cells. Immunoblots of the load (L), FT, and IP fractions were probed with antibodies to acetylated tubulin, detyrosinated tubulin, and polyglutamylated tubulin. Scale = 9 μm.

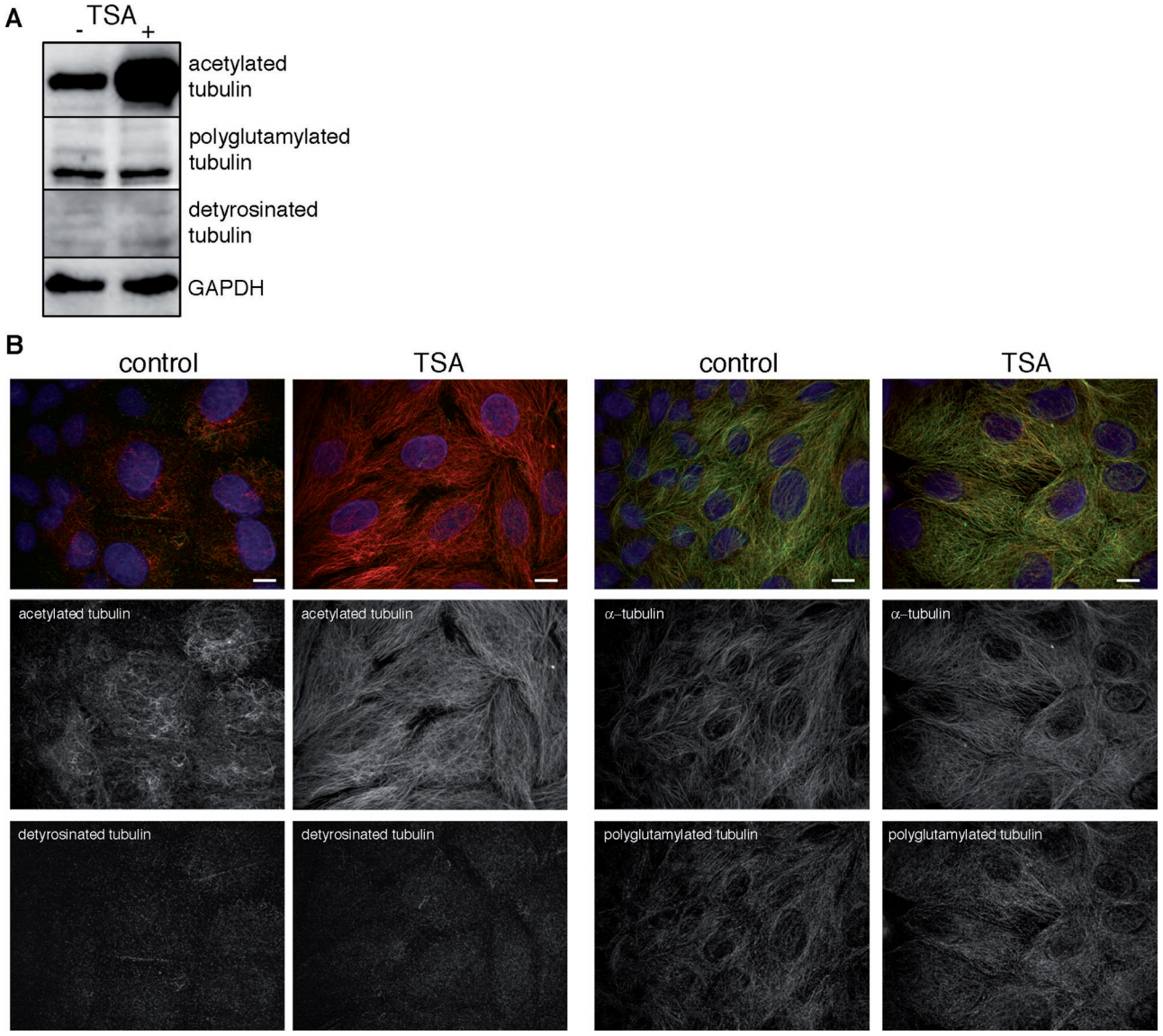


FIGURE 5: Hyperacetylation does not lead to an increase in detyrosinated tubulin or polyglutamylated tubulin. (A) Confluent MDCK cells were treated with the HDAC6 inhibitor TSA (+) or ethanol as a vehicle control (−) for 4 h and then lysed for immunoblotting with antibodies to acetylated tubulin, detyrosinated tubulin, polyglutamylated tubulin, and GAPDH as a loading control. (B) Cells were treated with TSA or ethanol as a vehicle control for 4 h and then fixed for immunocytochemistry with antibodies to acetylated tubulin (red) and detyrosinated tubulin (green) (left panels), or α-tubulin (green) and polyglutamylated tubulin (red) (right panels). All cells were counterstained with DAPI (blue). Scale = 9 μm.

different populations of microtubules, but also that these microtubules have different dynamic and perhaps functional characteristics.

## DISCUSSION

Here we have shown that tubulin PTMs demarcate multiple subpopulations of microtubules in MDCK epithelial cells. The conventional understanding is that there are dynamic microtubules that are unmodified and stable microtubules that are modified. A logical extension of this understanding is that, if a microtubule is stable, it should have all the modifications present in the cell. It has previously been shown that some cells do not display certain tubulin modifications, either because they do not express the appropriate modification enzyme or because that enzyme is silenced in some way (Bulinski *et al.*, 1988), but here we have shown that the same cell can have microtubules expressing single modifications or different combinations of modifications. These data suggest that tubulin modifications do not simply occur on all stable microtubules, but that some degree of regulation controls which microtubules are modified by which enzymes.

We have also shown that microtubule subpopulations differ in cells at different stages of polarity. Spreading cells that have a two-dimensional polarity have high amounts of all three modifications examined, but detyrosinated microtubules are more prominent than either acetylated or polyglutamylated microtubules, and these detyrosinated microtubules often point to the spreading edge. As cells undergo morphogenesis and acquire apical–basal three-dimensional polarity, the microtubule cytoskeleton undergoes a transition from a predominantly centrosomal array to a complex assemblage of noncentrosomal arrays (Müsch, 2004; Bartolini and Gundersen, 2006;

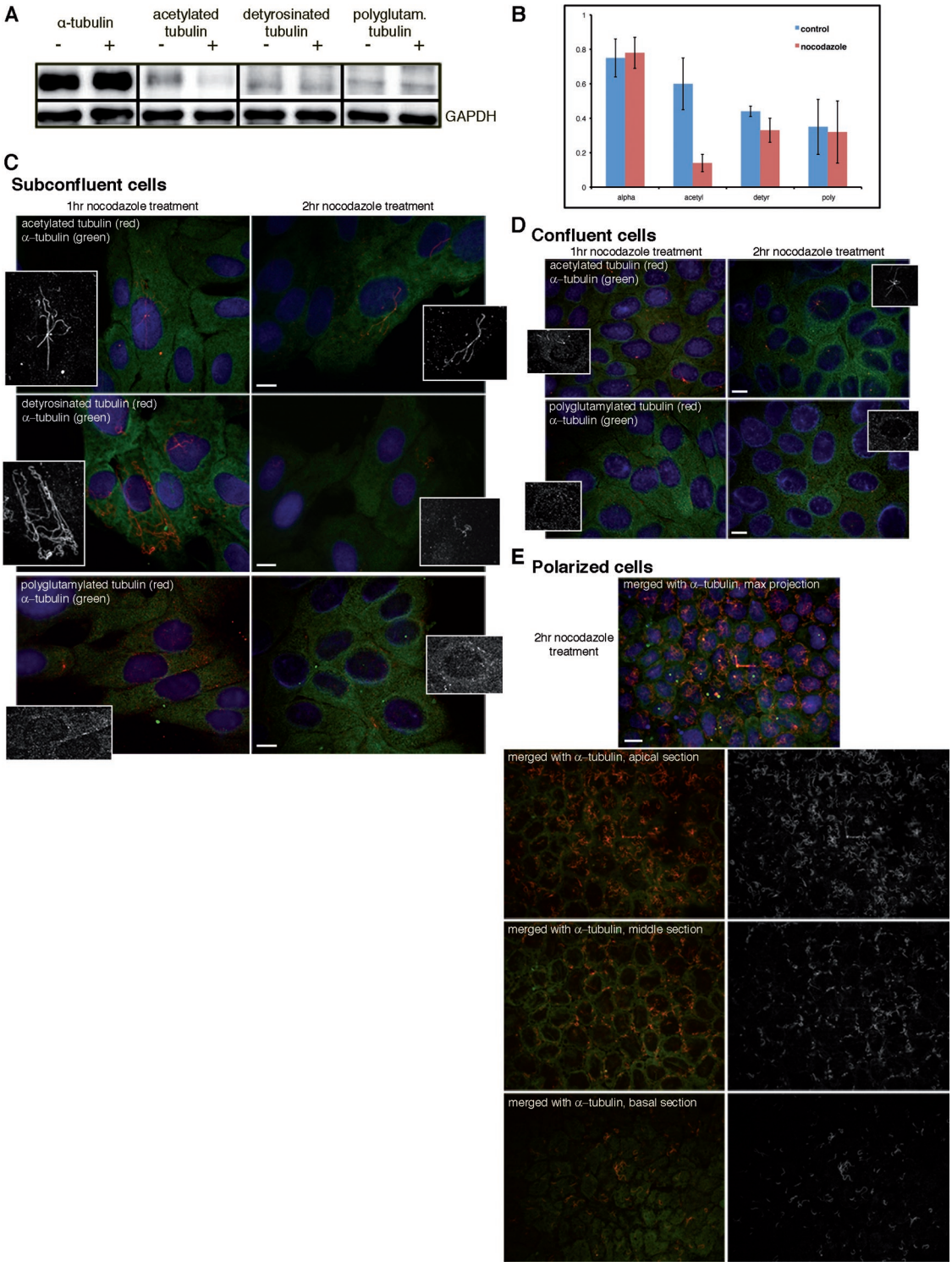


FIGURE 6: Microtubules with different PTMs show different sensitivity to nocodazole-induced depolymerization. (A) Confluent MDCK cells were incubated with 33 μM nocodazole (+) or DMSO as a vehicle control (−) for 1 h and then lysed and immunoblotted with antibodies to α-tubulin, acetylated tubulin, detyrosinated tubulin, polyglutamylated tubulin, and GAPDH as a loading control. (B) Densitometric quantification of lysates (n = 3 independent lysates for each condition). Subconfluent (C) or confluent (D) cells were incubated with 33 μM nocodazole for 1 or 2 h, then fixed and prepared for immunocytochemistry with antibodies to α-tubulin (green) in combination with acetylated tubulin, detyrosinated tubulin, or polyglutamylated tubulin (red) and were counterstained with DAPI (blue). In each case, insets showing representative cells with only the tubulin PTM labeling are shown as well. (E) Polarized cells were incubated with 33 μM nocodazole for 2 h, then fixed and prepared for immunocytochemistry with antibodies to α-tubulin (green) and acetylated tubulin (red) and counterstained with DAPI (blue). In all cases, control (DMSO)-treated cells were indistinguishable from untreated (as in Figures 2 and 3). Scale = 9 μm.

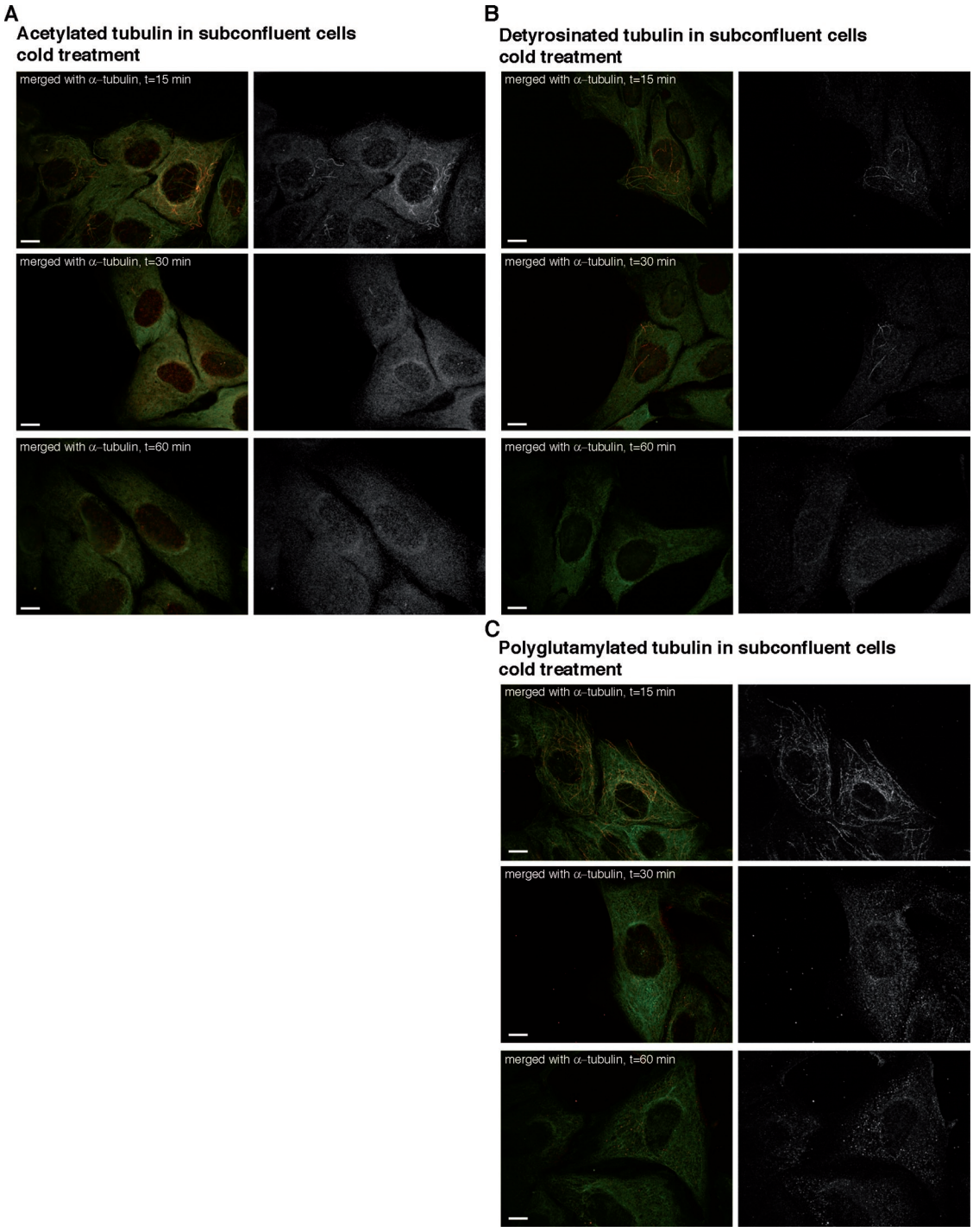


FIGURE 7: Microtubules with different PTMs show different sensitivity to cold-induced depolymerization. Subconfluent MDCK cells were incubated at 4°C for 15, 30, or 60 min, then fixed and prepared for immunocytochemistry with antibodies to α-tubulin (green) in combination with acetylated tubulin (red) (A), detyrosinated tubulin (red) (B), or polyglutamylated tubulin (red) (C). In all cases, control cells (kept at 37°C) were indistinguishable from untreated cells (as in Figures 2 and 3). Scale = 9 μm.

Tanos and Rodriguez-Boulan, 2008; Weisz and Rodriguez-Boulan, 2009). Here we show that the PTM of tubulin also changes with polarization. Tubulin detyrosination and polyglutamylation decrease substantially, and acetylated microtubules become more prominent. Further experiments are needed, however, to determine whether the change in polarity or microtubule reorganization leads to the change in tubulin modification and whether the changes in modification lead to polarization and/or microtubule reorganization.

These data also suggest that there are different degrees of stability and that stability does not directly correlate with PTMs. Furthermore microtubules may differ in their stability to drug- and cold-induced depolymerization. Treatment with nocodazole causes the depolymerization of all polyglutamylated microtubules (in subconfluent cells, where all three modifications are expressed at relatively high levels) and all but a few acetylated microtubules, but many of the detyrosinated microtubules persist. These detyrosinated

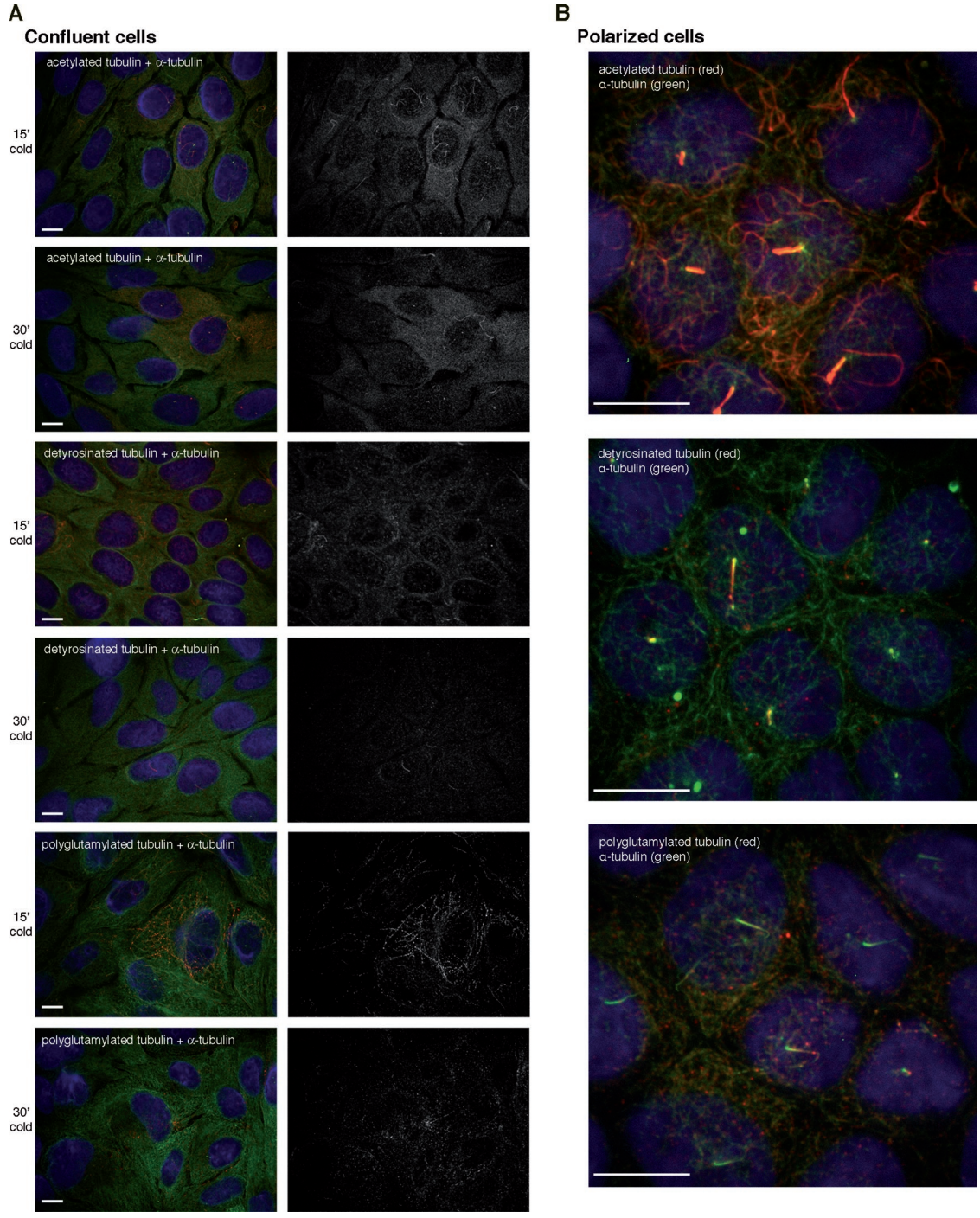


FIGURE 8: Microtubules with different PTMs in confluent and polarized cells also show different sensitivity to cold-induced depolymerization. (A) Confluent MDCK cells were incubated at 4°C for 15 or 30 min, then fixed and prepared for immunocytochemistry with antibodies to α-tubulin (green) in combination with acetylated tubulin (red) (first two rows), detyrosinated tubulin (red) (middle two rows), or polyglutamylated tubulin (red) (bottom two rows). (B) Polarized MDCK cells were incubated at 4°C for 15 min, then fixed and prepared for immunocytochemistry with antibodies to α-tubulin (green) in combination with acetylated tubulin (red) (top), detyrosinated tubulin (red) (middle), or polyglutamylated tubulin (red) (bottom). Shown are maximum projection images. In all cases, control cells (kept at 37°C) were indistinguishable from untreated cells (as in Figures 2 and 3). Scale = 9 μm.

microtubules are not permanently stable, as they are depolymerized by longer drug treatment. Interestingly, a few acetylated microtubules do persist after a 2-h nocodazole treatment, suggesting that they may represent a small hyperstable population. Cold incubation, however, produced different results. In subconfluent cells, short cold incubations led to the depolymerization of all but a few detyrosinated microtubules, but many acetylated microtubules and polyglutamylated microtubules persisted. Further experiments will be necessary to clarify the difference between drug and cold stability and the relationship between these stable microtubules and PTMs. Interestingly, recent evidence has suggested that tubulin PTMs may target microtubules for spastin-mediated severing as

well, which would also affect microtubule stability (Lacroix *et al.*, 2010). Together these data suggest that the microtubule population in the cell is complex, with individual microtubules varying in their constellation of modifications and dynamic properties. This complexity may support a wide range of functional diversity in the microtubule network, including, but not limited to, providing a range of navigational cues for molecular motors.

Although it is clear that some molecular motors show an increased affinity for microtubules that have been posttranslationally modified, it remains unclear which of the PTMs motors prefer. Some data have suggested that kinesin-1 family motors prefer to walk along microtubules that are detyrosinated (Konishi and Setou, 2009), whereas others have suggested that the motors prefer acetylated microtubules (Reed *et al.*, 2006; Hammond *et al.*, 2010). Many of these experiments have been performed in neurons, where PTMs are highly coordinated (Banerjee, 2002). It is possible that motors prefer a combination of PTMs, or prefer different PTMs under different regulatory conditions. Experiments in cells such as these in which PTMs are not highly coordinated may help to elucidate the mechanisms underlying motor preference.

The microtubule network in both two- and three-dimensional polarized epithelial cells has a complex organization, and molecular motors must be able to interpret directional cues to deliver cargo to appropriate domains. In two-dimensionally polarized cells, such as migrating cells and spreading cells, cargo must be delivered to the leading edge, and our data suggest that detyrosinated microtubules may serve as the tracks for this traffic. In three-dimensionally polarized cells, much of the secretory traffic is directed toward the apical domain, and our data suggest that acetylated microtubules of the longitudinal bundles and apical mesh may serve as the tracks for this traffic. These data suggest that either different motors that prefer different microtubule tracks are involved in cargo transport at different stages of polarization or that a regulatory switch takes place in motor preference. It has been shown that different motors are involved in vesicular transport in unpolarized versus polarized cells (Jaulin *et al.*, 2007; Xue *et al.*, 2010), but further experiments are needed to determine if the motor change, the track change, or both are necessary.

## MATERIALS AND METHODS

### Cell culture

MDCK epithelial cells were grown according to standard protocols in DMEM (HyClone, Logan, UT) with 10% fetal bovine serum. Cells were grown to the subconfluent (<50% confluence), confluent (95–100% confluence), or polarized stage (cultured for 48–72 h after reaching confluence and visually confirmed to have undergone the morphogenic changes stereotypical of polarity). Some cells were grown on Costar Transwell membrane inserts (0.4 μm pore size) (Corning, Lowell, MA) until fully polarized.

### Cell lysates and immunoblotting

Cells at the appropriate stage were scraped into RIPA buffer (50 mM Tris-HCl, 150 mM NaCl, 2 mM EDTA, 1% Triton X-100, 0.1% SDS, 0.25% sodium deoxycholate, pH 8.0) with added protease inhibitors (1% vol/vol of protease inhibitor cocktail for mammalian cells; Research Products International, Mt. Prospect, IL) on ice. Lysates were then cleared by centrifugation at 13,000 × *g* for 5 min at 4°C and an equal volume of 2× denaturing sample buffer (0.125% bromophenol blue, 25% glycerol, 2.5% SDS in 0.2 M Tris-HCl, pH 6.8 + 40 mM dithiothreitol) was added to the supernatant. Lysates were then separated by SDS–PAGE, and proteins were transferred to PVDF membranes (Millipore, Billerica, MA). Immunoblots were probed with antibodies to α-tubulin (DM1A; Sigma, St. Louis, MO), acetylated tubulin (6–11B-1; Sigma), detyrosinated tubulin (polyclonal; Millipore), polyglutamylated tubulin (B3; Sigma), Δ2 tubulin (polyclonal; Millipore), or GAPDH (Sigma) as a loading control. Blots were quantified by densitometric analysis using ImageJ (National Institutes of Health, Bethesda, MD, http://rsb.info.nih.gov/ij/). The integrated area of each band was normalized to the integrated area of the GAPDH band on the same blot. The ratio of the normalized posttranslationally modified tubulin to the normalized α-tubulin was then calculated for each sample. Pairwise Student's *t* tests were performed to determine if the relative amount of each modified tubulin differed significantly between stages of polarization. For one set of samples labeled with a detyrosinated tubulin antibody, a line was drawn perpendicular to the bands, and the intensity profile along the band was plotted using ImageJ to show the relative intensity and distribution of multiple bands.

### Immunocytochemistry

Cells were grown on glass coverslips to the appropriate stage and then fixed by immersion in methanol + 1 mM EGTA at –20°C for 10 min or immersion in methanol/EGTA at –20°C for 10 min followed by immersion in acetone at –20°C for 10 min. (used primarily for labeling with the polyglutamylated tubulin antibody). Coverslips were then air-dried, rinsed in phosphate-buffered saline (PBS), pH 7.4, and incubated in blocking solution (5% normal goat serum, 1% bovine serum albumin in PBS) before antibody incubation. Some cells (in particular coverslips with polarized cells and filter-grown cells) were fixed by incubation in 3.7% paraformaldehyde/0.05% glutaraldehyde in PHEM (20 mM PIPES, 7.5 mM HEPES, 4.5 mM EGTA, 1 mM $MgCl_2$) + 0.5% Triton X-100 at 37°C for 10 min, followed by a rinse in PHEM/Triton + 10% dimethyl sulfoxide (DMSO) and quenching with 50 mM $NH_4Cl$ in PBS. Cells were then rinsed in PBS and incubated in blocking solution as mentioned earlier in the text. Immunocytochemistry was performed with antibodies described earlier in the text, and cells were counterstained with DAPI to label nuclei. Comparisons and test immunocytochemistry experiments were performed to ensure that the different fixation protocols resulted in similar overall cell morphologies and microtubule network structures, although individual epitope availability varied between the different conditions. Quantification of fluorescence images was performed by drawing an ROI (region of interest) around the cell periphery and measuring the integrated fluorescence for each label using Volocity software (Improvision/PerkinElmer, Waltham, MA) and normalizing to the integrated α-tubulin signal. Linescans along microtubules were performed in ImageJ.

### Immunoprecipitation

Lysates were prepared as described earlier in the text, then precleared by overnight incubation with Protein-G Sepharose beads (GenScript, Piscataway, NJ). Precleared lysates were considered the "load" fraction. Acetylated tubulin antibody was bound to Protein-G Sepharose beads, and precleared lysates were incubated with antibody-bound beads on ice overnight. The beads were pelleted by centrifugation, and the supernatant was collected as the "flow-through" fraction. The beads were washed four times with PHEM buffer, and the washes were collected as wash fractions. After the final wash, the beads were resuspended in an equal volume of 2× sample buffer. Samples were separated by SDS–PAGE, and immunoblots were performed as described earlier in the text.

### Drug and cold treatments

For the TSA experiments, cells were grown to the appropriate stage and then treated with 5 μM TSA (Cell Signaling Technology, Beverly,

MA) or 0.1% ethanol (vehicle control) for 4 h before lysis or fixation for immunocytochemistry as described earlier in the text. For the nocodazole experiments, cells were incubated with 33 μM nocodazole (Sigma) or with 0.1% DMSO (vehicle control) for 1 or 2 h before lysis or fixation. For the cold exposure experiments, cells were transferred to medium containing 40 mM HEPES 30 min prior to the experiment to buffer the pH. The culture plate was then transferred to a 4°C incubator for 15, 30, or 60 min before fixation or lysis.


## ACKNOWLEDGMENTS

We thank Megan Salt and Seyfullah Kotil for preliminary experiments on this project. Partial funding for this research was provided by RAMP-Up! at Rensselaer: An NSF ADVANCE Initiative.


## REFERENCES


Astanina K, Jacob R (2010). KIF5C, a kinesin motor involved in apical trafficking of MDCK cells. Cell Mol Life Sci 67, 1331–1342.

Bacallao R, Antony C, Dotti C, Karsenti E, Stelzer EH, Simons K (1989). The subcellular organization of Madin-Darby canine kidney cells during the formation of a polarized epithelium. J Cell Biol 109, 2817–2832.

Banerjee A (2002). Coordination of posttranslational modifications of bovine brain alpha-tubulin. Polyglycylation of delta2 tubulin. J Biol Chem 277, 46140–46144.

Bartolini F, Gundersen GG (2006). Generation of noncentrosomal microtubule arrays. J Cell Sci 119, 4155–4163.

Bré MH, Pepperkok R, Hill AM, Levilliers N, Ansorge W, Stelzer EH, Karsenti E (1990). Regulation of microtubule dynamics and nucleation during polarization in MDCK II cells. J Cell Biol 111, 3013–3021.

Bulinski JC, Richards JE, Piperno G (1988). Posttranslational modifications of alpha tubulin: detyrosination and acetylation differentiate populations of interphase microtubules in cultured cells. J Cell Biol 106, 1213–1220.

Cai D, McEwen DP, Martens JR, Meyhofer E, Verhey KJ (2009). Single molecule imaging reveals differences in microtubule track selection between Kinesin motors. PLoS Biol 7, e1000216.

Cereijido M, Robbins ES, Dolan WJ, Rotunno CA, Sabatini DD (1978). Polarized monolayers formed by epithelial cells on a permeable and translucent support. J Cell Biol 77, 853–880.

Eddé B, Rossier J, LeCaer JP, Desbruyères E, Gros F, Denoulet P (1990). Posttranslational glutamylation of alpha-tubulin. Science 247, 83–85.

Friedman JR, Webster BM, Mastronarde DN, Verhey KJ, Voeltz GK (2010). ER sliding dynamics and ER-mitochondrial contacts occur on acetylated microtubules. J Cell Biol 190, 363–375.

Gundersen GG, Bulinski JC (1988). Selective stabilization of microtubules oriented toward the direction of cell migration. Proc Natl Acad Sci USA 85, 5946–5950.

Gundersen GG, Kalnoski MH, Bulinski JC (1984). Distinct populations of microtubules: tyrosinated and nontyrosinated alpha tubulin are distributed differently in vivo. Cell 38, 779–789.

Hammond JW, Cai D, Verhey KJ (2008). Tubulin modifications and their cellular functions. Curr Opin Cell Biol 20, 71–76.

Hammond JW, Huang CF, Kaech S, Jacobson C, Banker G, Verhey KJ (2010). Posttranslational modifications of tubulin and the polarized transport of kinesin-1 in neurons. Mol Biol Cell 21, 572–583.

Jacobson C, Schnapp B, Banker GA (2006). A change in the selective translocation of the Kinesin-1 motor domain marks the initial specification of the axon. Neuron 49, 797–804.

Jaulin F, Xue X, Rodriguez-Boulan E, Kreitzer G (2007). Polarization-dependent selective transport to the apical membrane by KIF5B in MDCK cells. Dev Cell 13, 511–522.

Konishi Y, Setou M (2009). Tubulin tyrosination navigates the kinesin-1 motor domain to axons. Nat Neurosci 12, 559–567.

L'Hernault SW, Rosenbaum JL (1985). Chlamydomonas alpha-tubulin is posttranslationally modified by acetylation on the epsilon-amino group of a lysine. Biochemistry 24, 473–478.

Lacroix B, van Dijk J, Gold ND, Guizetti J, Aldrian-Herrada G, Rogowski K, Gerlich DW, Janke C (2010). Tubulin polyglutamylation stimulates spastin-mediated microtubule severing. J Cell Biol 189, 945–954.

Müsch A (2004). Microtubule organization and function in epithelial cells. Traffic 5, 1–9.

Nagasaki T, Chapin CJ, Gundersen GG (1992). Distribution of detyrosinated microtubules in motile NRK fibroblasts is rapidly altered upon cell-cell contact: implications for contact inhibition of locomotion. Cell Motil Cytoskeleton 23, 45–60.

Noda Y, Okada Y, Saito N, Setou M, Xu Y, Zhang Z, Hirokawa N (2001). KIFC3, a microtubule minus end-directed motor for the apical transport of annexin XIIIb-associated Triton-insoluble membranes. J Cell Biol 155, 77–88.

Piperno G, Fuller MT (1985). Monoclonal antibodies specific for an acetylated form of alpha-tubulin recognize the antigen in cilia and flagella from a variety of organisms. J Cell Biol 101, 2085–2094.

Piperno G, LeDizet M, Chang XJ (1987). Microtubules containing acetylated alpha-tubulin in mammalian cells in culture. J Cell Biol 104, 289–302.

Redeker V, Levilliers N, Schmitter JM, Le Caer JP, Rossier J, Adoutte A, Bré MH (1994). Polyglycylation of tubulin: a posttranslational modification in axonemal microtubules. Science 266, 1688–1691.

Reed AA *et al*. (2010). CLC-5 and KIF3B interact to facilitate CLC-5 plasma membrane expression, endocytosis, and microtubular transport: relevance to pathophysiology of Dent's disease. Am J Physiol Renal Physiol 298, F365–F380.

Reed NA, Cai D, Blasius TL, Jih GT, Meyhofer E, Gaertig J, Verhey KJ (2006). Microtubule acetylation promotes kinesin-1 binding and transport. Curr Biol 16, 2166–2172.

Tanos B, Rodriguez-Boulan E (2008). The epithelial polarity program: machineries involved and their hijacking by cancer. Oncogene 27, 6939–6957.

Thompson WC (1977). Post-translational addition of tyrosine to alpha tubulin in vivo in intact brain and in myogenic cells in culture. FEBS Lett 80, 9–13.

Verhey KJ, Hammond JW (2009). Traffic control: regulation of kinesin motors. Nat Rev Mol Cell Biol 10, 765–777.

Wang Y *et al*. (2003). Cytoplasmic dynein participates in apically targeted stimulated secretory traffic in primary rabbit lacrimal acinar epithelial cells. J Cell Sci 116, 2051–2065.

Waterman-Storer CM, Salmon ED (1997). Actomyosin-based retrograde flow of microtubules in the lamella of migrating epithelial cells influences microtubule dynamic instability and turnover and is associated with microtubule breakage and treadmilling. J Cell Biol 139, 417–434.

Weisz OA, Rodriguez-Boulan E (2009). Apical trafficking in epithelial cells: signals, clusters and motors. J Cell Sci 122, 4253–4266.

Xue X, Jaulin F, Espenel C, Kreitzer G (2010). PH-domain-dependent selective transport of p75 by kinesin-3 family motors in nonpolarized MDCK cells. J Cell Sci 123, 1732–1741.